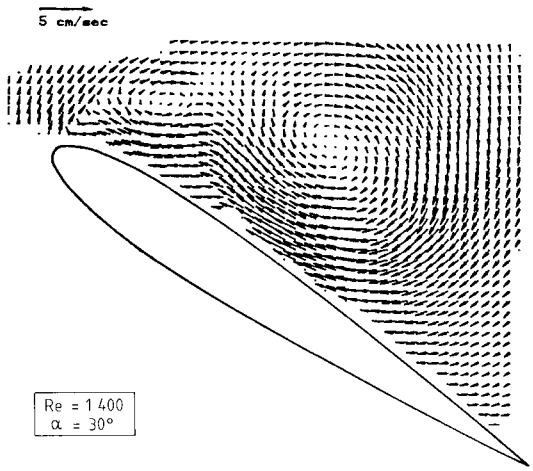

Fig. 3 Instantaneous velocity field over a NACA 0012 airfoil.

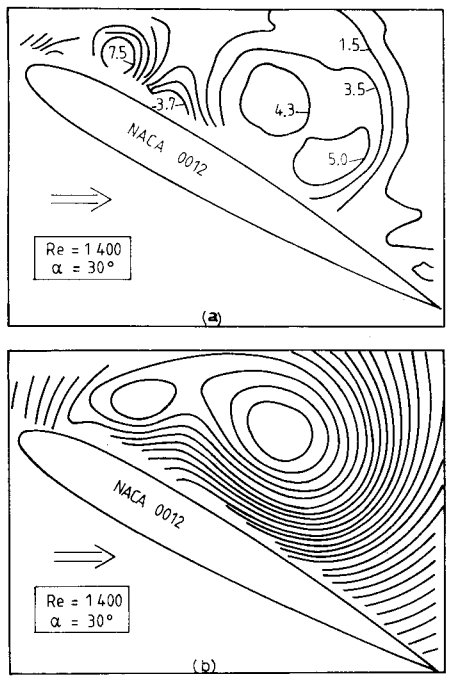

Fig. 4 Flow over NACA 0012 airfoil: a) isovorticity contours, b) streamline pattern.

For the boundaries of the velocity field, an excentered scheme is used to evaluate the spatial derivatives. Figure 4a displays the vorticity contours. An improved representation of the flowfield is obtained using the stream function (Fig. 4b). The later is computed using the vorticity values and integrating the Poisson equation. The features of this flowfield, for the Reynolds number presented here and for angles of attack greater than 15 deg, can be described as follows. First, a starting vortex is created at the trailing edge and sheds immediately downstream. This process occurs for $t^* < 0.1$. Concomitant with this, the flow at the leading edge separates and forms a closed recirculating bubble. This bubble is then convected downstream (large vortex in Fig. 3) as a vortex along the upper surface of the airfoil. This vortex is accompanied on its upstream side by another small vortex, as shown in Fig. 3. Similar observations were made by other investigators using conventional visualization techniques. However, Figs. 3 and 4 show vividly the quantitative velocity field and associated vorticity, along with a clear definition of the location of the vortex centers, vortex size, and the flow separation and reattachment points.

Conclusion

Particle image displacement velocimetry is a cost effective way to provide both quantitative and qualitative information of two-dimensional flowfields. This method is well suited to evaluate the velocity and vorticity distribution in unsteady flows and the data obtained may be used to gather both temporal and spatial information. Therefore, it is expected that this technique will permit a more detailed study of complex flowfields.

References

[1]Lourenco, L.M. and Krothapalli, A., "The Role of Photographic Parameters in Laser Speckle or Particle Image Displacement Velocimetry," *Experiments in Fluids*, to be published.

[2]Lourenco, L.M. and Krothapalli, A., "The Development of Laser Speckle or Particle Image Displacement Velocimetry, Part 1: The Role of Photographic Parameters," Florida State University, Tallahassee, Rept. FMRL-TR-1, 1985.

[3]Simpkins, P.G. and Dudderar, T.D., "Laser Speckle Measurements of Transient Bénard Convection," *Journal of Fluid Mechanics*, Vol. 89, 1978, pp. 665-671.

[4]Meynart, R., "Speckle Velocimetry Study of a Vortex Pairing in a Low Re Number Unexited Jet," *The Physics of Fluids*, Vol. 26, 1983, pp. 2077-2079.

[5]Lourenco, L.M. and Whiffen, M.C., "Laser Speckle Methods in Fluid Dynamics Applications," Paper presented at International Symposium on Application of Laser Velocimetry to Fluid Mechanics, Lisbon, 1984.

[6]Adrian, R.J. and Yao, C.S., "Development of Pulsed Laser Velocimetry for the Measurement of Fluid Flow," *Proceedings of Eighth Biennial Symposium on Turbulence*, Rolla, MO, 1984.

Multiple-Scale Turbulence Model in Confined Swirling Jet Predictions

C. P. Chen*
NASA Marshall Space Flight Center
Huntsville, Alabama

Introduction

In the last decade, advances have been made in turbulence modeling such that it is now possible to predict mean and turbulence characteristics of many shear flows. Among the models, the so called k-ϵ model has been shown to be adequate in a variety of flows.[1] However, in complex flows, such as confined swirling flows, the k-ϵ model is known to be deficient[2] due to the neglect of anisotropy in the turbulent viscosity and additional turbulence generation arising from streamline curvature. Several recent proposals,[3,4] which modify the k-ϵ model based on the streamline curvature Richardson numbers, give improved predictions in only certain limited regions of the swirling flow.[5,6] The purpose of this Note is to present a recently developed multiple-scale turbulence model, which seeks to circumvent deficiencies of earlier models by taking into account the nonequilibrium spectral energy transfer. The validity of this model is tested by predicting the confined swirling coaxial jet flow in a sudden expansion.

Received Oct. 25, 1985; revision received March 3, 1986.

*NRC-NASA Research Associate, Fluid Dynamics Branch, System Dynamics Laboratory.

Turbulence Model

Turbulence effects, which enter the governing equations, are modeled through a gradient-type approximation. Because of the nonequilibrium energy spectrum of the swirling flow, the eddy viscosity is represented by a multiple-scale turbulence model. A basic feature of this model is the partition of energy spectrum. This would allow the energy transfer of energetic eddies to be modeled based on the properties of the large scale flow characteristics, such as mean velocity gradients and degree of swirl, while the dissipation rate is related to the energy transfer by its own action rather than to the overall kinetic energy.

Two transport equations are provided representing the evolution of turbulent energy associated with the production range of the energy spectrum k_p and the transfer region of the energy spectrum k_t. To close these equations, two transport equations for the energy transfer rate across the spectrum are derived. The dissipation rate of the energetic eddies ϵ_p, is interpreted as the energy transfer rate from the energy-containing eddy motion. The dissipation rate of the small eddies, ϵ_t, is related to the energy transferred by its own action in the high wave number region of the spectrum. The modeled transport equations are summarized here (in cylindrical coordinates):

$$\frac{\partial Uk_p}{\partial x}+\frac{1}{r}\frac{\partial}{\partial r}(rVk_p)=\frac{\partial}{\partial x}\left(\frac{\nu_t}{\sigma_{k_p}}\frac{\partial k_p}{\partial x}\right)+\frac{1}{r}\frac{\partial}{\partial r}\left(\frac{r\nu_t}{\sigma_{k_p}}\frac{\partial k_p}{\partial r}\right)+G-\epsilon_p \tag{1}$$

$$\frac{\partial Uk_t}{\partial x}+\frac{1}{r}\frac{\partial}{\partial r}(rVk_t)=\frac{\partial}{\partial x}\left(\frac{\nu_t}{\sigma_{k_t}}\frac{\partial k_t}{\partial x}\right)+\frac{1}{r}\frac{\partial}{\partial r}\left(\frac{r\nu_t}{\sigma_{k_t}}\frac{\partial k_t}{\partial r}\right)+\epsilon_p-\epsilon_t \tag{2}$$

$$\frac{\partial U\epsilon_p}{\partial x}+\frac{1}{r}\frac{\partial}{\partial r}(rV\epsilon_p)=\frac{\partial}{\partial x}\left(\frac{\nu_t}{\sigma_{\epsilon_p}}\frac{\partial \epsilon_p}{\partial x}\right)+\frac{1}{r}\frac{\partial}{\partial r}\left(r\frac{\nu_t}{\sigma_{\epsilon_p}}\frac{\partial \epsilon_p}{\partial r}\right)+\frac{1}{\tau_p}[C_{p_1}G-C_{p_2}\epsilon_p] \tag{3}$$

$$\frac{\partial U\epsilon_t}{\partial x}+\frac{1}{r}\frac{\partial}{\partial r}(rV\epsilon_t)=\frac{\partial}{\partial x}\left(\frac{\nu_t}{\sigma_{\epsilon_t}}\frac{\partial \epsilon_t}{\partial x}\right)+\frac{1}{r}\frac{\partial}{\partial r}\left(r\frac{\nu_t}{\sigma_{\epsilon_t}}\frac{\partial \epsilon_p}{\partial r}\right)+\frac{1}{\tau_p}[C_{t_1}\epsilon_p-C_{t_2}\epsilon_t] \tag{4}$$

The quantity G in Eqs. (1) and (3) is the production of energy-containing eddies by the mean gradients, $\tau_p=k_p/\epsilon_p$, and σ_{k_p}, σ_{k_t}, σ_{ϵ_p}, σ_{ϵ_t}, C_{p_1}, C_{p_2}, C_{t_1}, and C_{t_2} are model coefficients.

The present multiple-scale model was developed based on the earlier version of Hanjalic et al.[7] and has been tested on several free shear and confined recirculating flows.[8] The details of the model development and established model coefficients can be found in these two papers. Using these model equations, the Reynolds stresses are expressed according to

$$\overline{u_i'u_j'}=-\nu_t\left[\frac{1}{2}\left(\frac{\partial U_i}{\partial x_j}+\frac{\partial U_j}{\partial x_i}\right)\right]+\frac{2}{3}k\delta_{ij}$$

where $k=k_t+k_p$ and the eddy viscosity is given by $\nu_t=C_\mu(k_p+k_t)(k_p/\epsilon_p)$ with $C_\mu=0.09$.

Numerical Results and Discussion

Numerical method, grid system, and boundary conditions used for computation are detailed in Ref. (9). The experimental work used to evaluate the turbulence model — a confined coaxial jet involving sudden expansion with swirl in the annular jet—is by Roback and Johnson.[10] The recirculation zone shape, formed in Roback and Johnson's experimental setup, is of type 3 (cf. Dixon et al.[11]), i.e., combination of a central reverse zone and an annular recirculation zone. This shape is faithfully mimicked by the multiple-scale model, as illustrated by a radial profile of mean axial velocities plotted in Fig. 1. The "three cell" flow structure at $x/D=0.21$ is correctly reproduced by the multiple-scale turbulence model. It is interesting to note that this flow structure cannot be predicted by a more complicated non-isotropic algebraic stress model, [cf. Ref. (6)].

Figure 2 compares radial profiles of mean tangential velocities at two downstream locations. The k-ϵ model has a more rapid decay of the swirl component than the multiple-scale model at the upstream location. However, both models

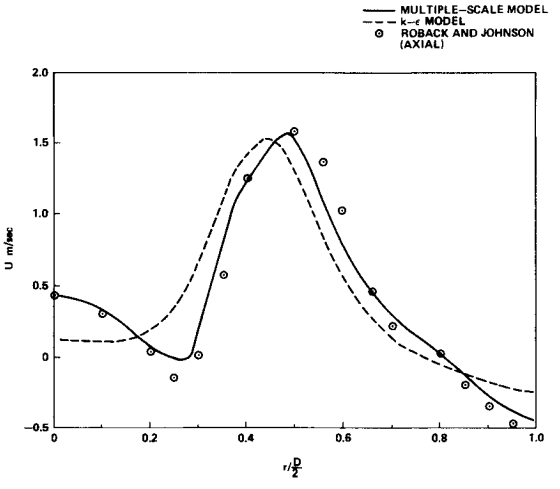

Fig. 1 Axial mean velocity profiles at $x/D=0.21$.

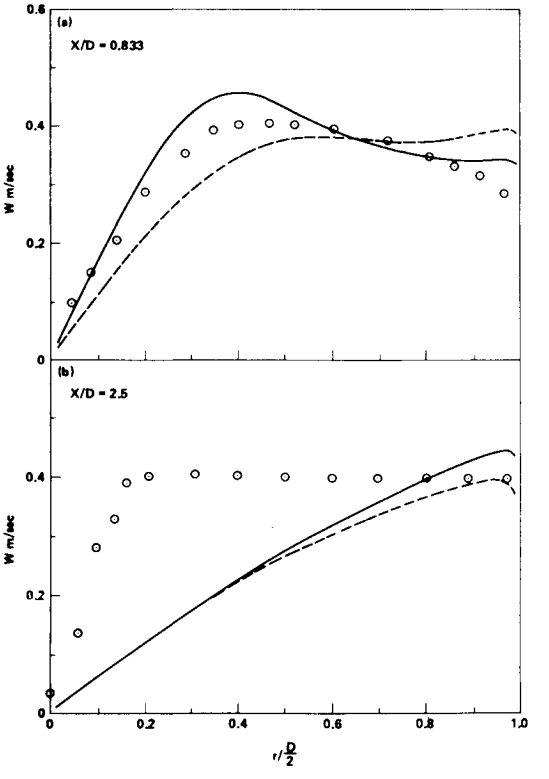

Fig. 2 Tangential mean velocity profiles at several downstream locations. Curves have the same meaning as Fig. 1.

predict tangential velocity decay for a solid-body rotation prematurely, while experimental data show a persistent combined vortex (i.e., combination of a free and forced vortex) profile even at the far downstream location. The discrepancies between the calculations and measurements indicate the deficiency of isotropic eddy viscosity hypothesis used in this level of closure. This discrepancy is also shared by the non-isotropic algebraic stress model (ASM) prediction.[6] As indicated by Sloan et al.,[6] the failure at the downstream location probably has to be resolved by solving the full stress transport equations, with convective and diffusive terms, rather than the abbreviated ASM.

More detailed comparisons, such as centerline mean velocity decay, envelope of the central recirculation zone, turbulence intensities, and the sensitivity of the numerical predictions to the inlet boundary conditions, have been documented in Ref. (9). The preliminary success of this model stems from recognizing that turbulence in swirl flows departs significantly from spectral equlibrium conditions and that the different energy transfer rates for energy-containing eddies and transfer eddies should be modeled separately. However, the multiple-scale model still adopts the isotropic eddy viscosity formulation. To account for anisotropic turbulence, a full Reynolds Stress Model needs to be used. Incorporation of the multiple-scale turbulence model, which takes into account the non-equilibrium spectral energy transfer rate, and a simplified Reynolds stress model should pave a promising avenue for numerical modeling of swirling flows.

Acknowledgment

This work was done while the author held a National Research Council-NASA Research Associateship. Financial support provided by NASA-MSFC and NRC is acknowledged. The comments of Dr. George Fichtl and the reviewers are also gratefully acknowledged.

References

[1]Rodi, W., "Examples of Turbulence Models for Incompressible Flows," *AIAA Journal*, Vol. 20, July 1982, pp. 872-879.

[2]Boysan, F. and Swithenbank, J., *Journal of Fluids Engineering*, Vol. 104, Sept. 1982, pp. 391-392.

[3]Launder, B. E., Pridden, C. H., and Sharma, B. I., "The Calculation of Turbulent Boundary Layers on Spinning and Curved Surface," *Journal of Fluid Engineering*, Vol. 88, March 1977, pp. 231-239.

[4]Rodi, W., "Influence of Buoyancy and Rotation on Equations for the Turbulent Length Scale," *Proceedings of 2nd Symposium on Turbulent Shear Flows*, Imperial College, London, pp. 10.37-10.42, July 1979.

[5]Chen, C. P., "Calculation of Confined Swirling Jets," *Commu. Applied Numerical Methods*, Vol. 2, 1986, pp. 333-338.

[6]Sloan, D, G., Smoot, L. D., and Smith, P. J., "Modeling of Swirl in Turbulent Flow Systems," Paper presented at Combustion Institute Spring Technical Meeting, Southwest Research Institute, San Antonio, TX, April 1985.

[7]Hanjalic, K., Launder, B. E., and Schiestel, R., "Multiple-Time-Scale Concepts in Turbulent Transport Modeling," *Turbulent Shear Flow II*, Springer-Verlag, NY, 1980, pp. 36-49.

[8]Chen, C. P., "Multiple-Scale Turbulence Modeling in Internal Flows," NASA CR-178536, submitted to *Physics of Fluids*, 1985.

[9]Chen, C.P., "Confined Swirling Jet Predictions Using a Multiple-Scale Turbulence Model," NASA CR-178484, Aug. 1985.

[10]Roback, R. and Johnson, B. V., "Mass and Momentum Turbulent Transport Experiments with Confined Swirling Coaxial Jets," NASA CR-168252, 1983.

[11]Dixon, T. F., Truelove, J. S., and Wall, T. F., "Aerodynamic Study on Swirled Coaxial Jets From Nozzles with Divergent Quarls," *Journal of Fluid Engineering*, Vol. 105, June 1983, pp. 197-203.

Analogy for Postbuckling Structural Resistance Capability

Elie Yitzhak* and Menahem Baruch†
Technion—Israel Institute of Technology, Haifa, Israel

Introduction

THE notion of static postbuckling analysis is contradictory. The use of static assumption presumes that accelerations and inertial forces remain inexistent during the loading process. On the other hand, sudden changes in the modes and rates of displacement, followed by different dynamic effects, are to be expected when buckling is about to occur. This contradiction makes questionable the ability of static analysis to provide actual information on postbuckling structural behavior. Therefore, the results usually supplied by static postbuckling analysis (i.e. the forces vs displacements diagrams) must be considered to be no more than estimations of the structure's ability to develop resistance forces when stability disappears.

Arguments similar to those expressed here have led several authors to inspect the possibility of performing dynamic postbuckling analyses in place of static ones.[1-3] The purpose of this Note is to point out that, in addition to the structural behavior history generally expected, it is possible to extract from the dynamic analysis results information such as diagrams of the structural resistance force vs displacement that are equivalent to the static postbuckling ones. In certain simple cases, diagrams from dynamic analyses are identical to those from static analyses. In more complicated cases, they will be different. Logically then, the dynamic analysis force vs displacement diagrams must contain better information about the structural strength capabilities. All of the existing theorems for the behavior of diagrams of static postbuckling analyses must also be valid for the equivalent dynamic analysis diagrams.

Example Case of Structural Instability

As an example, the assumption noted above will be applied to the case of the structural instability of an elastoplastic thin spherical pressure vessel (Fig. 1). This problem has already been treated from a classical static point of view by Durban and Baruch.[4] The static behavior of such a structure is analogous in many aspects to a nonstable postbuckling history without bifurcation. It is noted that the critical point is obtained on the load displacement path when the load reaches its maximum value. (Real structures, due to their imperfections, do not buckle generally by bifurcation and have a similar behavior to the spherical pressure vessel of this example.)

The internal pressure p is supposed to increase as a monotonic function of the time variable t,

$$p=\alpha t \qquad (\alpha=\text{const}) \tag{1}$$

Two different kinds of forces act together against this pressure: the structural resistance ρ, which represents the resultant of the existing membrane stresses σ within the structure, and an inertia pressure q:

$$\rho=2\sigma\frac{h_0+\eta}{r_0+u} \tag{2a}$$

Received Dec. 4, 1984; revision received Jan. 6, 1986.

*Graduate Student, Department of Aeronautical Engineering.
†Professor and Dean, Department of Aeronautical Engineering. Member AIAA.